université
PARIS-SACLAY

NNT : ***

n°LAL : ***

Search of the $0\nu\beta\beta$ decay with the SuperNEMO demonstrator

Thèse de doctorat de l'Université Paris-Saclay
préparée à l'Université Paris Saclay au sein du Laboratoire Irène-Joliot Curie
(anciennement Laboratoire de l'Accélérateur Linéaire)

École doctorale n°576 Particles, Hadrons, Energy, Nuclei, Instrumentation, Imaging, Cosmos et Simulation (PHENIICS)
Spécialité de doctorat : Physique des particules

Thèse présentée et soutenue à Orsay, le ***, par

CLOÉ GIRARD-CARILLO

Composition du Jury :

***	
***	Président
***	
***	Rapporteur
***	
***	Rapporteur
Christine Marquet CENBG - Bordeaux-Gradignan	Examinateur
***	
***	Examinateur
***	
***	Examinateur
Laurent Simard LAL - Orsay	Directeur de thèse
Mathieu Bongrand LAL - Orsay	Co-directeur de thèse

Thèse de doctorat

Contents

Chapter 6

Sensitivity of the SuperNEMO demonstrator to the $0\nu\beta\beta$

In this chapter, we present the SuperNEMO sensitivity to the search of $0\nu\beta\beta$ decay, and the corresponding effective neutrino masses, for several isotopes. The SuperNEMO final detector is expected to exclude $0\nu\beta\beta$ half-lives up to 1.2×10^{26} y (90% CL) if $0\nu\beta\beta$ decays through the exchange of a light Majorana neutrino, with a detector exposure of 500 kg.y [7]. The sensitivity is given as a limit, in case we do not observe the expected signal. In 2010 began the demonstrator installation at the Laboratoire Souterrain de Modane. With an exposure of 17.5 kg.y, the demonstrator could set a limit on the $0\nu\beta\beta$ process of 5.35×10^{24} y (90% CL) [8].

This study aims to explore the impact on the sensitivity of the presence of a magnetic field, and will participate in the final decision on the installation of the coil. In a context of investigating the demonstrator and final detector capabilities, different internal source contamination levels are explored. The topology of interest is the two electrons topology, and we use the $2e$ energy sum to discriminate the signal from the background events. Thanks to SuperNEMO tracking capabilities, topological informations are exploited to improve the SuperNEMO sensitivity.

6.1 Signal and background simulations

A full simulation for the SuperNEMO demonstrator was perfomed, in order to determine the longest $0\nu\beta\beta$ half-life that can be probed with SuperNEMO using the distribution of the sum of electron energies, in the case where the $0\nu\beta\beta$ decay were not observed. In the Tab. 6.1 is summarised the expected number of signal and background events, both for the SuperNEMO demonstrator and final detector, and we present the size of Monte-Carlo simulations for each isotope.

The $0\nu\beta\beta$ signal

In the following, the assumed underlying mechanism for the $0\nu\beta\beta$ decay exist through the exchange of a light Majorana neutrino, the so-called mass mechanism (MM), as it is the most natural and widespread mechanism. The hypotetical $0\nu\beta\beta$ signal would be detected as an excess of events in the region of interest, with

	Expected decays		Simulated decays
	Demonstrator	Final detector	
$0\nu\beta\beta$ ($T^{0\nu}_{1/2} = 2.5\,10^{23}$ y)	$3.6\,10^2$	$1.0\,10^4$	$1.0\,10^7$
$2\nu\beta\beta$	$9.5\,10^5$	$2.7\,10^7$	$1.0\,10^7$
^{208}Tl	$5.5\,10^3$	$1.6\,10^5$	$1.0\,10^7$
^{214}Bi	$1.1\,10^3$	$3.1\,10^4$	$1.0\,10^7$
^{222}Rn	$1.8\,10^5$	$7.2\,10^6$	$1.0\,10^7$

Table 6.1: Expected and simulated decays for different processes, both for the demonstrator (17.5 kg.y) and for the final detector (500 kg.y), assuming target background activities are reached. The $T^{0\nu}_{1/2}$ value is given only illustratively: the decay has never been observed, so we choose the limit on the half-life obtained with NEMO-3 [ref]. Exepected number of events are given not taking into account the cut efficiencies, and in the full energy range. We remind the target activities: $\mathcal{A}^{\mathrm{Tl}} = 10\,\mu$Bq.kg, $\mathcal{A}^{\mathrm{Bi}} = 2\,\mu$Bq.kg, $\mathcal{A}^{\mathrm{Rn}} = 0.15$ mBq.m^{-3}

respect to the predicted background contamination level. The 10^7 $0\nu\beta\beta$ Monte-Carlo events are generated using the DECAY0 software [9]. The simulations are normalised assuming a $T^{0\nu}_{1/2} = 6.0\,10^{24}$ y half-life [citation].

Inside detector backgrounds

In the full energy range, the allowed $2\nu\beta\beta$ decay stands as the dominant internal background type. However, beyond a certain value in energy, the number of $2\nu\beta\beta$ events decreases very quickly, because of the energy spectrum shape. Moreover, its contribution is reduced if the half-life increases, and is enhanced if the energy resolution is worsened. To offset this effect, we simulated 10^7 $2\nu\beta\beta$ decays inside the source foils, with a total energy > 2 MeV, in addition of the normal $2\nu\beta\beta$ decays. ($T^{2\nu}_{1/2} = 9.39 \pm 0.17$ (stat) ± 0.58 (syst) $\times 10^{19}$ years from the NEMO-3 experiment [10]), and we normalised the total $2\nu\beta\beta$ spectrum. As described in Sec. 3.2.1, source foil contaminations by isotopes such as ^{208}Tl or ^{214}Bi constitute the principal internal backgrounds with the $2\nu\beta\beta$ decay. These backgrounds are processed by the same detector simulation as the $0\nu\beta\beta$ signal, using DECAY0. Since internal backgrounds have very low efficiencies in the $2e$ topology, we simulated an important amount of Monte-Carlo events.

A component of the external background producing events similar to the internal background is caused by the presence of ^{222}Rn inside the tracking detector volume, and constitute a separate background category. If such an decay occurs on or near a foil and appears with a $2e$ topology, it becomes hard to distinguish from a double beta decay candidate. This isotope being distributed throughout the whole tracking detection volume, it was therefore necessary to simulate a large quantity of this isotope in the detector to maximise the amount of ^{214}Bi events, coming from ^{222}Rn decays, in the region of interest.

The target background activities detailed in Sec. 3.2 were defined so that each background has a similar contribution to that of the $2\nu\beta\beta$ in the region of interest [11]. We remind these nominal in Tab. 6.2, and give a comparison with the measured activities of the demonstrator source foils contaminations, as well as a measurement of the ^{222}Rn activity inside the tracker volume.

	Nominal activities	Real activities
^{208}Tl	$10\,\mu$Bq.kg^{-1}	$54\,\mu$Bq.kg^{-1}
^{214}Bi	$2\,\mu$Bq.kg^{-1}	$< 290\,\mu$Bq.kg^{-1}
^{222}Rn	0.15 mBq.m^{-3}	0.15 ± 0.02 mBq.m^{-3} [12]

Table 6.2: Real and targeted nominal activities for the SuperNEMO detector.

Outside detector backgrounds

This background category is due to the external γ-ray flux produced by radioactive isotope decays in detector components or surrounding laboratory rocks, as well as neutron interactions in the shield and of the detector's material. The limit on external background number of counts set by the NEMO-3 experiment was < 0.2 in the $2e$ total energy range [2.8 - 3.2] MeV, for an exposure of 34.3 kg·y [13]. Thus, we consider all external backgrounds from outside the foil, apart from ^{222}Rn in the tracking volume, are expected to be negligible and were not simulated. The most notorious difference is the fact that the SuperNEMO scintillator blocks are thicker than those of NEMO-3, and so a gamma is less likely to cross a scintillator without interacting. Therefore, for the same PMTs radioactivity, Radiopurity measurement for SuperNEMO PMTs allow to conclude that the total activity of SuperNEMO PMTs is better than for NEMO-3, for the two principal considered isotopes ^{208}Tl and ^{214}Bi [14].

We select only events matching the $2e$ toplogy. As a reminder, a reconstructed particle is tagged as an electron if it has a negatively curved track with a vertex on the source foils and an associated calorimeter hit. Energy spectra of all processes presented above are displayed in Fig. 6.1. In the following we present an optimisation of the event selection and of the region of interest.

6.2 Optimisation of event selection

Most of the double beta experiments are only sensitive to the total electron energy sum. Such a variable is presented in Fig. 6.1 in logarithmic scale, for each simulated process detailed in Sec. 6.1. The total number of events for each decay represent the amount of selected $2e$ topologies. The $0\nu\beta\beta$ spectrum is peaked around 2.8 MeV, the $Q_{\beta\beta} = 2.99$ MeV energy being degraded by electron energy losses, explaining the asymetric energy distribution. The progeny of ^{222}Rn produces γ-rays and β decays accompanied by internal conversion (IC), Møller or Compton scattering,

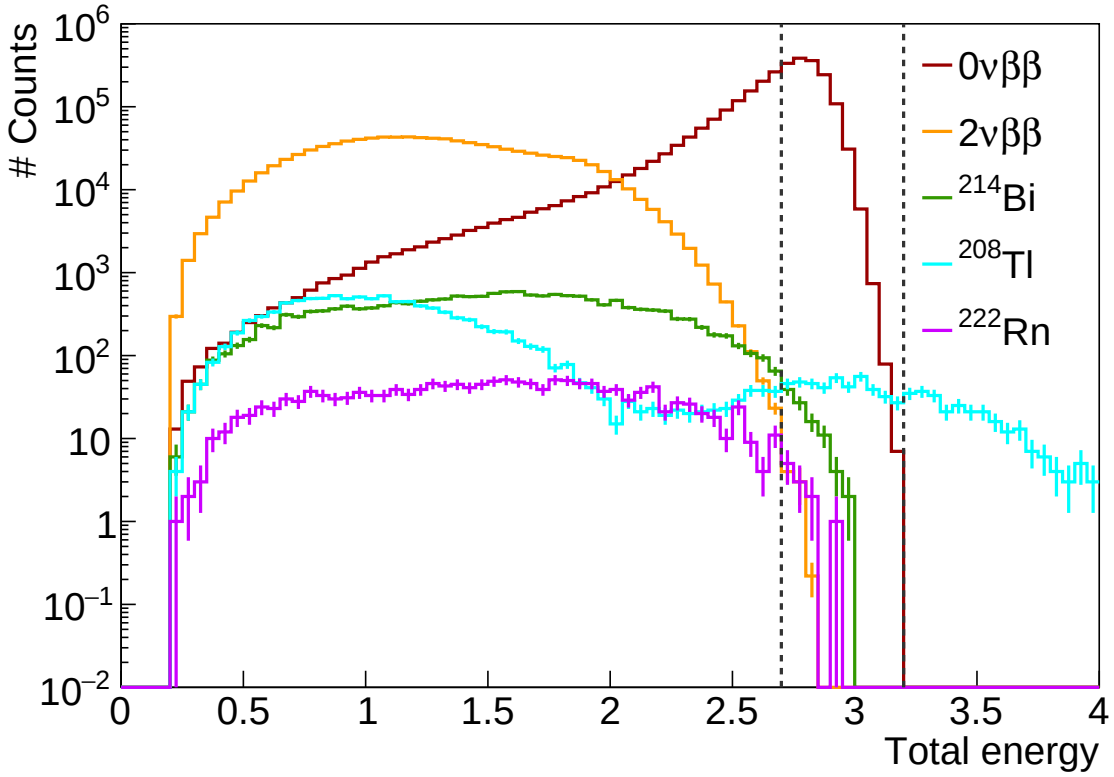

Figure 6.1: Energy spectra for the $0\nu\beta\beta$ signal and for the main backgrounds. The region of interest, whose optimisation is discussed in Sec. 6.2, is matarialised by two dashed vertical lines. ^{208}Tl events dominate in the ROI.

the dominant mechanism being the first one. ^{214}Bi and ^{222}Rn energy distributions have the same variations, ^{214}Bi being one of the descendents of ^{222}Rn.

Tab. 6.3 sums up the expected number of counts in the full energy range as well as in the region of interest.

	Full energy range	[2.75;2.85] MeV
$0\nu\beta\beta$	$2.7\,10^{6}$	$9.5\,10^{-2}$
$2\nu\beta\beta$	$9.1\,10^{5}$	$1.1\,10^{-1}$
^{208}Tl	$1.7\,10^{4}$	9.9^{-3}
^{214}Bi	$1.1\,10^{4}$	$2.7\,10^{-2}$
^{222}Rn	$1.1\,10^{4}$	

Table 6.3: Real and targeted nominal activities for the SuperNEMO detector.

To allow the selection of $0\nu\beta\beta$ signal events while rejecting a high proportion of background events, topological cuts have been set up, in addition with the basical cuts described above (negatively curved track, a vertex on source foil and an associated calorimeter). These cuts are designed to reject events where the two

electrons are not emitted simultaneously, or from the same location on the source foil, and hence have a high rejection efficiency for ^{222}Rn events.

- $P_{int} > 4\%$:
  The internal probability, based on TOF computation, is detailed in Sec. 4.0.1. The chosen level insures that non simultaneous events are rejected.

- $\Delta y < 60$ mm and $\Delta z < 70$ mm:
  The two reconstruted vertices on source foils should not be separated by more than 60 mm horizontally, and by more than 70 mm vertically, to maximise the selection of two electrons emitted at the same spot.

These cuts follow the NEMO-3 analysis on the external background rejection, whose effectiveness were lately confirmed for the SuperNEMO demonstrator [15].

The integrated efficiency spectra, computed by comparing the number of selected events to the number of Monte Carlo events, are presented in Fig. 6.2. Once computed, the efficiency of selection helps finding the number of background

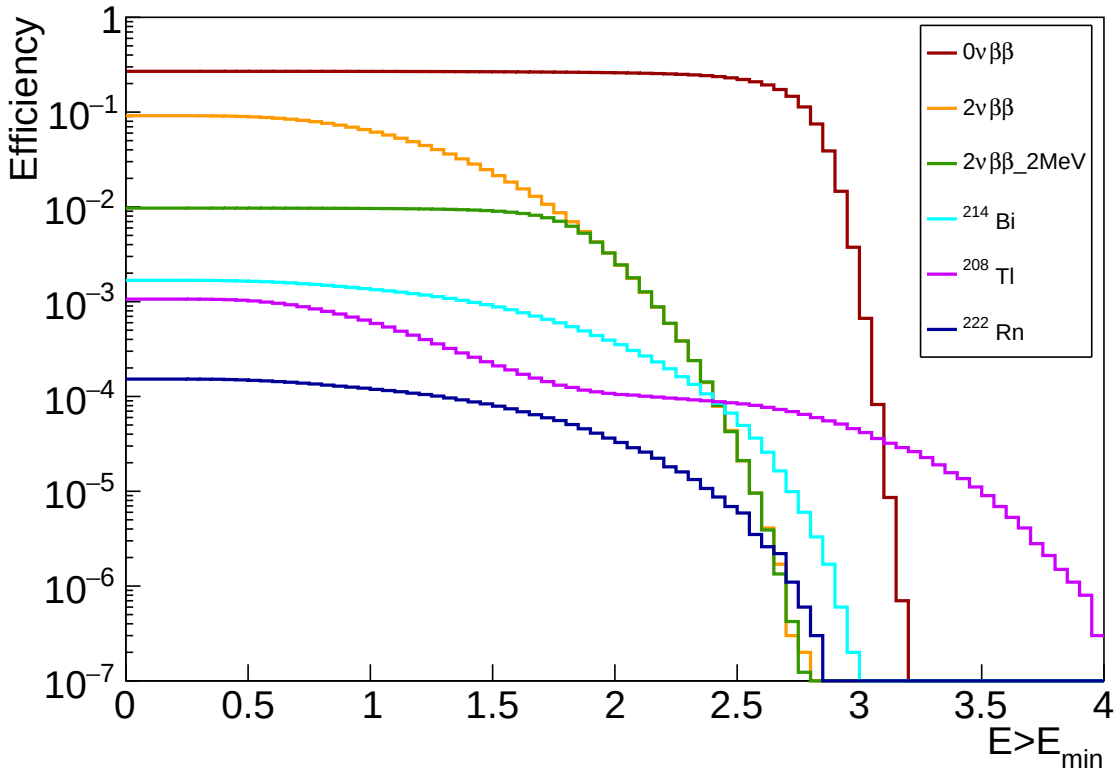

Figure 6.2: Efficiency spectra for $E > E_{min}$, for the $0\nu\beta\beta$ signal and for the main backgrounds.

events expected, for $E > E_{min}$, presented in Fig. 6.3.

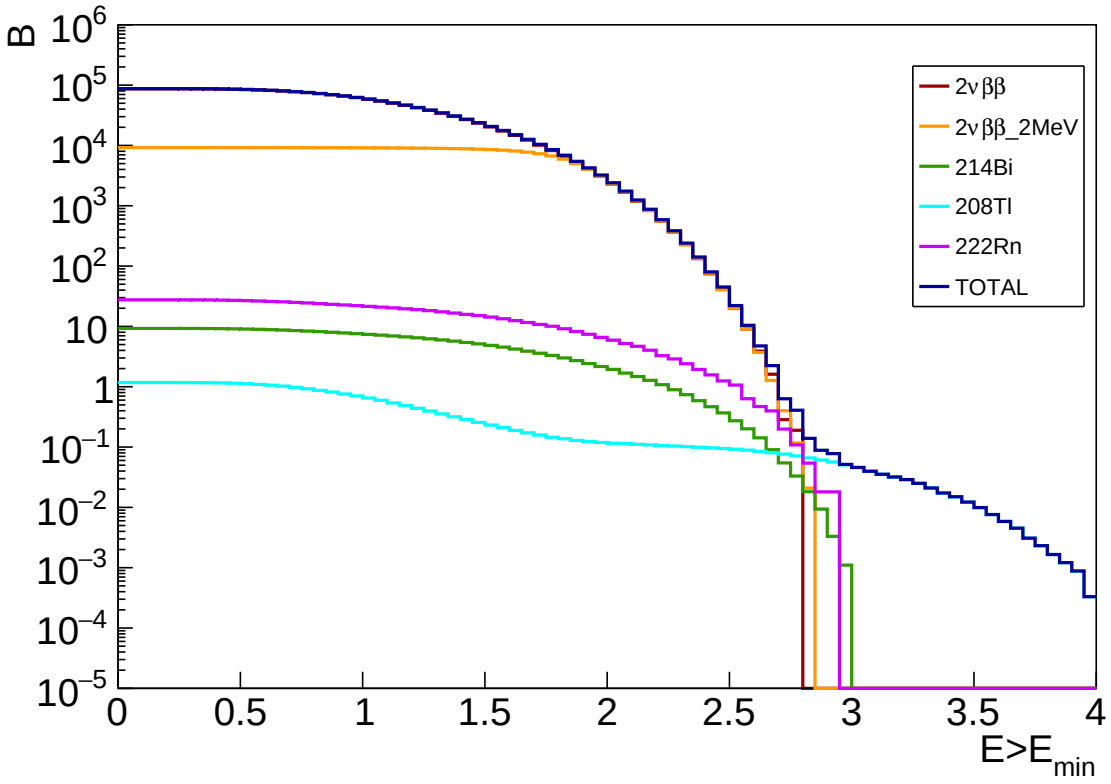

Figure 6.3: Expected number of background events, for $E > E_{min}$.

6.3 Expected number of background events

The number of background expected in a given energy window

$$\mathcal{N} = \frac{\mathcal{N}_a \log 2}{M_{\mathrm{Se}}} \times \frac{\epsilon m t}{T^{2\nu}_{1/2}} \tag{6.1}$$

depends on the number of ^{82}Se atoms composing the source foils, the detection efficiency ϵ in this energy window, the exposure mt and the $2\nu\beta\beta$ decay half-life $T^{2\nu}_{1/2}$.

- plot energy tot
- plus dans région intéret

6.4 Demonstrator sensitivity

- Résultats $B = 0$, avec activités nominales, puis avec activités caca
- Efficiency spretra
- Energy spectra
- Influence des quantités de contaminations sur la sensibilité

6.4.1 avec B

Parler du champ non uniforme/attenuation ROI optimization: avec variation coupure énergie

6.4.2 sans B

avec variation coupure énergie

6.4.3 Champ mappé

6.5 HyperNEMO

results for 500kg.y exposure

6.6 Other isotopes

distribution t1/2 avec différents échantillons de simus (17.5 kg.y)

6.7 Conclusion

- Etude plus générale avec bkg externe+lab (reprendre chiffres NEMO3) + neutrons (cf NEMO3)
- Plot général récap tous résultats
- delayed cells-¿improvement, cf NEMO 3

Bibliography

[1] M. et al. Agostini. Probing majorana neutrinos with double-β decay. *Science 365*, 1445, 2019.

[2] S.I. et al Alvis. Search for neutrinoless double-beta decay in ^{76}ge with 26 kg-yr of exposure from the majorana demonstrator. *Phys. Rev. C*, 100, 2019.

[3] O. et al. Azzolini. First result on the neutrinoless double-β decay of ^{82}Se with cupid-0. *Phys. Rev. Lett.*, 120:232502, Jun 2018.

[4] C. et al. Alduino. First results from cuore: A search for lepton number violation via $0\nu\beta\beta$ decay of ^{130}Te. *Phys. Rev. Lett.*, 120:132501, Mar 2018.

[5] J. B. et al. Albert. Search for neutrinoless double-beta decay with the upgraded exo-200 detector. *Phys. Rev. Lett.*, 120:072701, Feb 2018.

[6] A. et al. Gando. Search for majorana neutrinos near the inverted mass hierarchy region with kamland-zen. *Phys. Rev. Lett.*, 117:082503, Aug 2016.

[7] R. et al. Arnold. Probing new physics models of neutrinoless double beta decay with supernemo. *Eur. Phys. J. C*, 2010.

[8] S. Clavez. *Development of reconstruction tools and sensitivity of the SuperNEMO demonstrator*. PhD thesis, Université Paris Sud, 2017.

[9] Tretyak V.I. Ponkratenko O.A. and Zdesenko Yu.G. The event generator decay4 for simulation of doublebeta processes and decay of radioactive nuclei. *Phys. At. Nucl.*, 63:1282–1287, Jul 2000.

[10] R. et al. Arnold. Final results on ^{82}se double beta decay to the ground state of ^{82}kr from the nemo-3 experiment. *Eur. Phys. J. C*, 2018.

[11] Gomez-Cadenas et al. Physics case of supernemo with ^{82}se source. Internal presentation, 2008.

[12] Xin Ran Liu. Radon mitigation strategy and results for the supernemo experiment. IoP APP / HEPP Conference, 2018.

[13] R. et al. Arnold. Results of the search for neutrinoless double-β decay in ^{100}mo with the nemo-3 experiment. *Phys. Rev. D*, 2015.

[14] Frédéric Perrot. Radiopurity measurements for 8" pmts and preliminary budget for the sn demonstrator. Internal presentation, 2017.

[15] Steven Calvez. Updates on the demonstrator sensitivity and radon study. Internal presentation, 2014.